JOURNAL OF OPTOELECTRONICS AND ADVANCED MATERIALS Vol. 8, No. 1, February 2006, p. 60 - 65

Microwave behaviour of ferrite composites

D. LISJAK[a*], V. B. BREGAR[a,b], A. ZNIDARSIC[b], M. DROFENIK[a]
[a]*Jozef Stefan Institute, Advanced Materials Dep., Jamova 39, SI-1000 Ljubljana, Slovenia*
[b]*Iskra Feriti d.o.o., a member of Kolektor group, Stegne 29, 1000 Ljubljana, Slovenia*

Three types of ceramic composites were prepared using solid-state reaction at 1000-1300°C: spinel/M-hexaferrite (SM), Z-hexaferrite/U-hexaferrite (ZU) and Z-hexaferrite/W-hexaferrite (ZW). The evolution of phases was studied with X-ray powder diffraction and the microstructures of the composites were examined with electron microscopy. Their microwave behaviour was studied with respect to their composition and microstructure. The permeabilities of composites were strongly influenced by the permeabilities of the constituent phases and their porosity. This was quantified using the effective-medium theory (EMT). The permeabilites that were calculated with EMT from permeabilities of single-phase samples were matched with measured effective permeability of composite samples. On the contrary, the initial permeability of W-hexaferrite was calculated from the permeability values obtained from the ZW composite. It is shown that EMT can be used for the quantitative characterization of permeability in ferrite composites.

(Received October 14, 2005; accepted January 26, 2006)

Keywords: Microwave, Ferrite, Ceramic, Composite

1. Introduction

The increasing exploitation of microwave (MW) frequencies for telecommunications has increased electromagnetic (EM) interference and pollution and stimulated the development of MW absorbers. Absorption of EM waves occurs in magnetic materials due to the magnetic losses. Ferrites exhibit substantial magnetic losses in the vicinity of their ferromagnetic resonance (FMR). Because of this they are one of the best materials for MW absorbers. Ferrites with a spinel crystal structure can be applied in the high-frequency region of several hundreds MHz to several GHz.[1] Spinel ferrites are ferrimagnetic oxides in the system Fe_2O_3-MO, where M = LiFe, Ni, MnZn, NiZn, CoNi, CoNiZn. The other type of materials, hexaferrites, can be used across the whole GHz region.[2] Hexaferrites are ferrites with complex crystal structures based on a magneto-plumbite structure in the system AO-Fe_2O_3-MeO, where A = Ba, Sr, Ca(La) and Me = a bivalent transition metal.[3] The most typical hexaferrites are the so-called M-type ($AFe_{12}O_{19}$), W-type ($AMe_2Fe_{16}O_{27}$), X-type ($A_2Me_2Fe_{28}O_{46}$), Y-type ($A_2Me_2Fe_{12}O_{22}$), Z-type ($A_3Me_2Fe_{24}O_{41}$) and U-type ($A_4Me_2Fe_{36}O_{60}$). The numerous ferrite chemical compositions and crystal structures make it possible to tailor their electromagnetic properties, such as the saturation magnetization, the magneto-crystalline anisotropy, the permittivity, and the permeability. The microstructure of the ferrites has an additional influence on their properties, like permittivity, permeability and consequently on the EM absorption. Therefore, in the development of suitable absorbers, their composition and processing are equally important.

Absorbers can be produced as ceramics or as composites. The EM properties of composites can be very effectively tuned, simply by varying the volume fractions of the constituent phases. In addition, a synergetic effect of the constituent phases' properties may also be observed in some composites. For this reason magnetic composites are interesting for microwave applications. The magnetic properties of composites are usually calculated using effective-media theories provided the appropriate quantities and equations are used. In this paper we will present the influence of composition and microstructure on microwave behaviour in composite systems: spinel/M-hexaferrite, Z-hexaferrite/U-hexaferrite and Z-hexaferrite/W-hexaferrite. We will show that for the composites studied, the modified effective-media model [4] can be applied, if the microstructure is taken into an account.

2. Experimental

Ferrite composites were prepared as ceramics with a solid-state reaction at 1000-1300 °C from raw oxides and carbonates. The spinel ferrite phase in the study was Ni ferrite (M = Ni), and the hexaferrites here were Ba-Co hexaferrites (A = Ba, Me = Co). Therefore, we will refer in this text to these phases as spinel and hexaferrites, respectively. Composites with various mass ratios of the two constituent phases were prepared. The conditions used for a particular composite preparation are listed in Table 1. Reactive sintering involves the preparation of composites that combines the formation of the constituent phases (by firing) and sintering at the same time.

Table 1. Preparation conditions for ferrite composites.

composite	constituent phases	Firing conditions	sintering conditions
SM	Ni ferrite M hexaferrite	1000 °C 1h 1300 °C 1h	1230 °C
ZU	Z hexaferrite U hexaferrite	1300 °C 6h	= reaction sintering
ZW	Z hexaferrite W hexaferrite	1300 °C 6h	= reaction sintering

The evolution of the phases was controlled with X-ray powder diffraction (XRD) using a D4 Endeavor diffractometer (Burker AXS) with $Cu_{K\alpha}$ radiation and with an energy-dispersive spectrometry (EDS) using a LINK ISIS system connected to a Jeol-5800 scanning electron microscope (SEM). The SEM was also used for microstructural observations of the composites. The density of the composites was calculated from the measured mass and dimensions. The relative sintering densities were calculated taking into an account the theoretical density of the spinels and hexaferrites, which is approximately 5.3 g/cm^3 for both and were 90% for the SM composites (including single phase spinel and M-hexaferrite), 70% for the ZU and 85% for the ZW composites. The mass ratio of the constituent phases, which were formed during the reaction sintering, was determined with a Rietveld refinement [5] or from the integral intensities of the XRD peaks from the diffractograms refined using the Pawley method [6] and the crystallographic program Topas2R 2000 from Bruker AXS, Karlsruhe, Germany. The diffractograms were refined using the space groups Fd3m (227) for the spinel, $P6_3/mmc$ (194) for the M, W- and Z-hexaferrite and R3m (166) for the U-hexaferrite. In this paper the second method will be, for the sake of simplicity, referred as the Pawley method, and the intensity will refer to the integral intensity.

The permeability of the materials was obtained by measuring the impedance with an HP 4291A Impedance Analyser (measurements were made from 1MHz to 1 GHz) and the S-parameters with an Anritsu 37369C Vector Network Analyser (measurements were made from 100 MHz to 10 GHz). With the latter method we also determined the permittivity of the materials. For both measurements the same short-circuited APC-7 coaxial line was used as the sample holder and the samples were machined to fit into the coaxial line. With such a measurement set-up there are no demagnetisation factors and the obtained permeability is the intrinsic permeability of the material. Therefore, we can use this permeability for the calculations with the effective medium equation. For determining the best match of the calculated effective permeability with the measured permeability and subsequently the relevant volume fractions of spinel and hexaferrite phases in the SM composites we compared the difference of the integrals of both permeabilities over 0.1–3.0 GHz frequency range. For hexaferrite composites initial permeabilities of the consitutent phases (μ_i) were calculated using the basic effective-media theory equation [4], where j refers to a particular phase j.

$$\sum_j F_j \frac{\mu_{i,j} - \mu_{i,efff}}{\mu_{i,j} + 2\mu_{i,eff}} = 0 \qquad (1)$$

3. Results and discussion

3.1 MS composites

Fig. 1 shows X-ray diffractograms of the SM composite and single phase spinel and M-hexaferrite, sintered at 1228 °C. The peaks in the diffractograms correspond only to the spinel structure in the case of spinel sample, only to the M-hexaferrite crystal structure in case of the M-hexaferrite sample and to both in case of the MS composite sample. The lattice parameters of the constituent phases are listed in Table 2. It is clear that they vary with the composites composition. This suggests that the compositions of the constituent phases deviate slightly with respect to the overall phase composition. According to known phase relations spinel and M-hexaferrite react to form W-hexaferrite ($BaMe_2Fe_{16}O_{27}$) [7]. This can explain the variations in the lattice parameters. The spinel lattice increased in the presence of the M-hexaferrite. Although, the a parameter of the M-hexaferrite varied less than the method's uncertainty the M-hexaferrite lattice decreased significantly in the c direction in the presence of the spinel phase. This must be a consequence of ions diffusion from the M-hexaferrite lattice to the spinel. Consequently, W-hexaferrite was formed, which was confirmed with the SEM and EDS analyses. Fig. 2 shows a backscattered-electron (BE) image of the SM composite with 30wt.% of spinel sintered at 1228 °C. Spinel, M- and W-hexaferrite phases were detected by the EDS. Clearly, the W-hexaferrite grains are very small, as is their amount. Therefore, the relevant peaks could not be observed in the X-ray diffractogram.

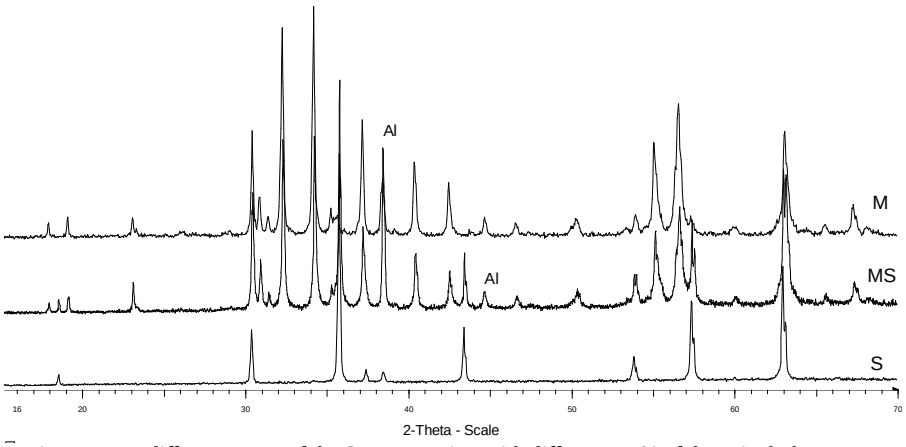

Fig. 1. X-ray diffractograms of the SM composites with different wt.% of the spinel phase.

Table 2. Lattice parameters of the spinel and M-hexaferrite in the SM composites sintered at 1228 °C.

spinel wt.%	spinel lattice parameters (Å)	M-hexaferrite lattice parameters (Å)
100	a = 8.3413(2)	/
30	a = 8.3424(1)	a = 5.8865(1) c = 23.199(1)
20	a = 8.3451(2)	a = 5.8857(1) c = 23.201(1)
10	a = 8.3534(3)	a = 5.8907(1) c = 23.217(1)
0	/	a = 5.8894(1) c = 23.214(1)

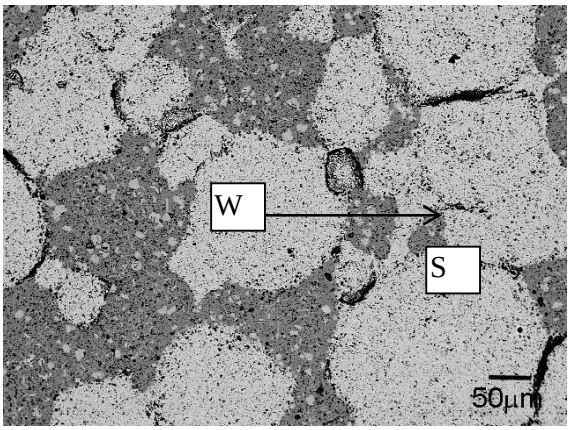

Fig. 2. BE image of the SM composite with 30 wt.% of spinel, sintered at 1228 °C. S denotes spinel, M and W denote M- and W-hexaferrite, respectively.

Since the permittivity is approximately the same for ferrite phases, we focused our analysis on the permeability, where the differences between the various phases can be significantly larger. Fig. 3 shows the permeability (μ) spectra of SM composites with different vol.% of the spinel phase (F), sintered at 1228 °C. In order to be able to compare μ between the composites of different composition, the porosity was strictly controlled, and was for all SM composites approximately 10 vol.% (see Experimetal part). Furthermore, the vol.% matches to the wt.% of each phase due to the equal densities of spinel and M-hexaferrite. The spinel phase exhibits a significant initial permeability and magnetic losses from 300 MHz up, which can be attributed to the mix of ferromagnetic resonance (FMR) and domain-wall relaxation (DWR). In contrast, the M-hexaferrite has its FMR at 50 GHz [2] and consequently, the magnetic losses and FMR contribution to the initial permeability is low. The observed magnetic losses and the higher intrinsic permeability can be attributed to the DWR; however, the total effective permeability in the observed frequency range is significantly lower than that of the spinel phase. Clearly, the μ spectra of the SM composites show the influence of both ferrimagnetic phases. As expected, the effective permeability of the composite increases with the mass proportion of spinel phase. Using the effective media theory the complex μ for SM composites of various compositions was calculated. The comparison between the experimental data and the data calculated on the basis of equation (1) for the sample with 20 wt.% of spinel are shown in Fig. 4. The best fit was obtained for 21.5 vol.% of spinel, which matches very well to the nominal composition of the sample and to the XRD quantitative phase analysis [8]. The small amount of W-hexaferrite formed during the sintering did not influence significantly on the μ of the SM composites. This is to be expected since the amount of W-hexaferrite was small and its μ is, as will be shown later, similar to the M-hexaferrite in the measured frequency region.

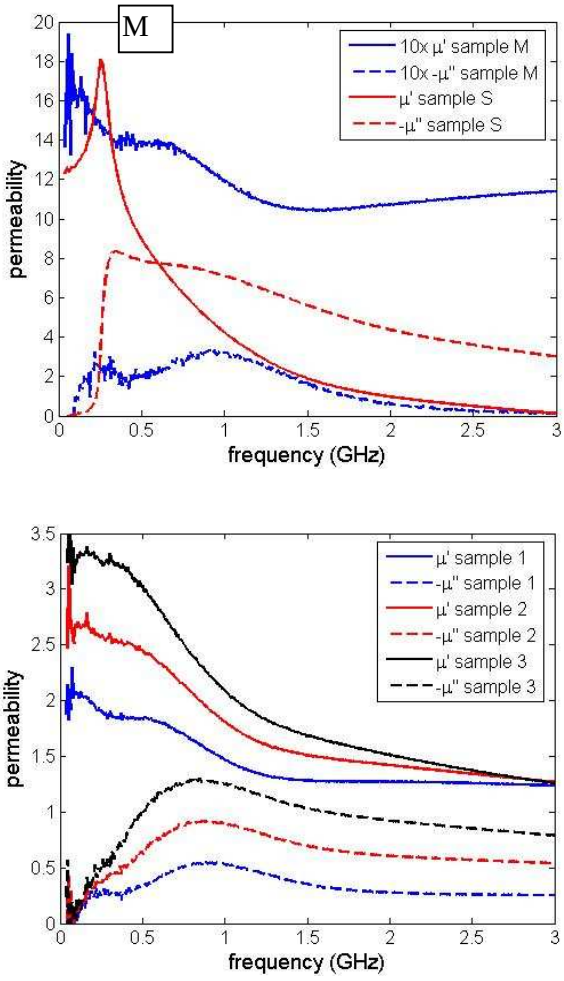

Fig. 3. Permeability spectra of the SM composites sintered at 1228 °C. Solid lines correspond to the real permeability μ' and the dotted lines to the imaginary permeability - μ''. For an easier comparison the permeability of sample M is multiplied by 10.

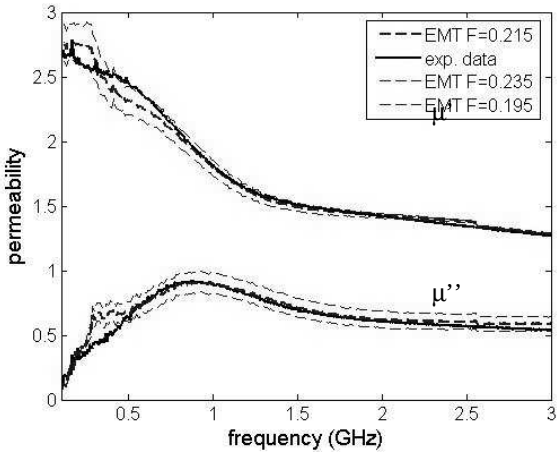

Fig. 4. Experimental data (solid line) and calculated (dashed lines) permeability (Eq. 1) with different volume fractions of spinel for a sample with the nominal composition of 20 wt.% .

3.2 Hexaferrite composites

Fig. 5 shows X-ray powder diffractograms of hexaferrite composites sintered at 1300 °C. The diffraction peaks of the ZU composites correspond to the Z- and U-hexaferrite structures and those of the ZW composite to the Z- and W-hexaferrite structures only. This confirms that the composites consisted of only two ferrimagnetic phases. The lattice parameters of the constituent phases are listed in Table 4. The difference in the lattice parameters of the Z-hexaferrite in the ZU and ZW composites indicates different compositions and/or site occupancies in the Z-hexaferrite lattice in each composite. Fig. 6 shows BE images of hexaferrite composites sintered at 1300 °C. Two phases corresponding to Z- and U-hexaferrite were detected with the EDS in the ZU composite; the grains are randomly oriented and have a diameter of 20 μm or more. Besides the two main phases, Z- and W-hexaferrite, two minor phases, spinel and Y-hexaferrite, were also detected with the EDS in the ZW composite. The grains of main phases are randomly oriented and several tens of μm large, while the grains of the minor phases are significantly smaller. The fractions of the minor phases were obviously below the detection limit of the XRD and were not observed in the X-ray diffractogram. Therefore, only the wt.% of the main phases were determined with the XRD, and they are listed in Table 4. Only the Pawley method was applied for the ZU composite since there is no published data on the U-hexaferrite structure. A minor discrepancy between the mass fractions determined with different XRD methods can be observed for the ZW composite. This discrepancy is roughly in the range of the determination error and can be attributed to the different basis of the methods used. The Rietveld method is based on the structure model and the peak intensities are fitted with respect to the structure and the mass ratios of the crystalline compounds in the sample. However, in the case of the hexagonal hexaferrite crystallites preferential orientation can be induced during the sample preparation for the XRD analysis and cannot be avoided or controlled. As a consequence, the intensities of the (0 0 l) and (h k 0) peaks (see Fig. 5) are also influenced by the degree of preferential orientation. In contrast, the Pawley method is based on the whole pattern decomposition and the peaks intensities are irrelevant and depend only on the mass ratios of the crystalline compounds in the sample. When the Pawley method was used, the (0 0 l) and (h k 0) peaks of the hexaferrite structure were omitted from the calculation.

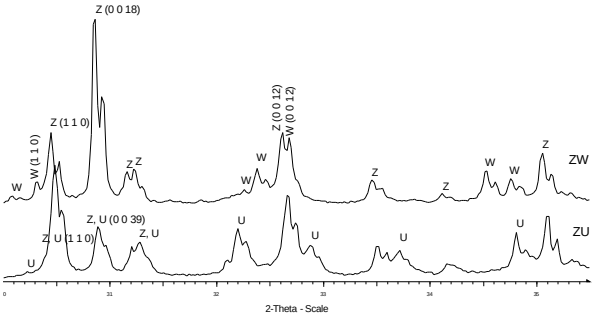

Fig. 5. X-ray diffractogram of the hexaferrite composites sintered at 1300 °C. For the sake of clarity only (h k 0) and (0 0 l) indeces are indicated.

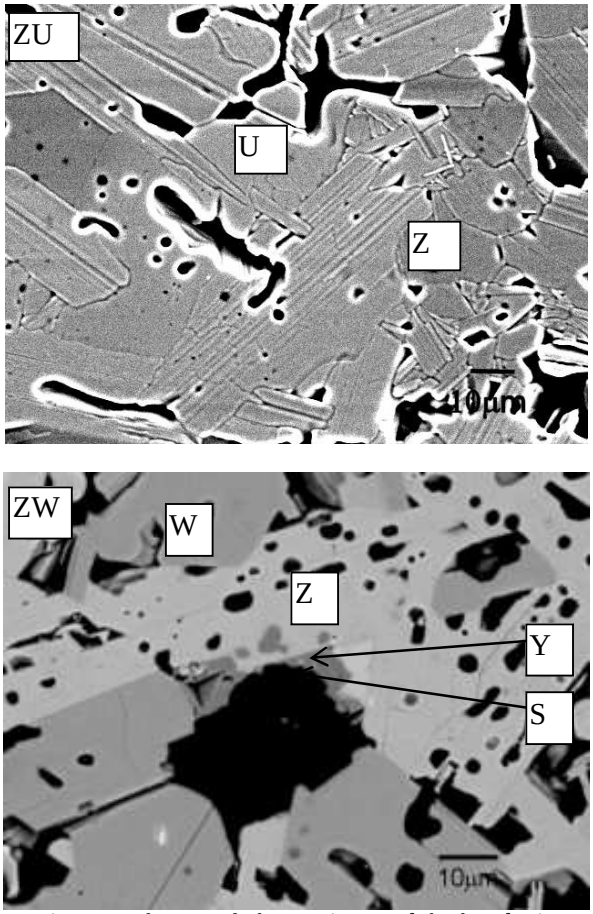

Fig. 6. Backscattered-electron image of the hexaferrite composites sintered at 1300 °C. Z, U, W, Y and S denote Z-, U-, W-, Y-hexaferrite and spinel, respectively.

Table 4. The amount (wt.%) of Z-hexaferrite phase in the ZU- and ZW-composites including their lattice parameters.

composite	wt. % Z Pawley method	wt% Z Rietveld method	Z lattice parameters (Å)	U / W lattice parameters (Å)
ZU	50	/	a = 5.852(1) c = 51.97(1)	a = 5.859(2) c = 112.55(4)
ZW	68	65	a = 5.873(2) c = 52.17(3)	a = 5.898(1) c = 32.88(3)

Fig. 7 shows the μ spectra of a ZU composite. An increase in magnetic losses and μ" can be observed around 1-2 GHz and above 8 GHz. The lower-frequency increase in μ" can be attributed to the DWR of both hexaferrites and to the FMR of the Z-hexaferrite [2,9,10]. The higher-frequency increase in μ" can be attributed to the FMR of the U-hexaferrite [11]. The difference in the FMR frequencies of the constituent phases is large enough so that they can be distinguished. The overlapping is only partial, as can be seen in Fig. 7. The μ_i measured at 40 MHz is approximately 5.8, which is lower than that reported for the Z-hexaferrite ceramics (μ_i ~ 11-12) [2,9,10] and higher than was measured for the U-hexaferrite ceramics (μ_i ~ 4.7) [11]. Using the effective-media equation (1) for μ_i of a composite, taking into account the porosity of the samples, the volume fractions of the Z- and U-hexaferrite phase were calculated. Here μ_i = 1 was taken for the air in the pores. According to the calculation, the ZU composite is composed of 42 vol.% Z-hexaferrite and 28 vol.% U-hexaferrite. This corresponds to 60 wt.% of Z-hexaferrite and to 40 wt.% of U-hexaferrite, which is not exactly consistent with the XRD-analysis (Table 4). For this particular case, the Pawley method is less reliable than the calculation based on Equation (1) due to a partial overlapping of the peaks corresponding to the two similar hexaferrite structures, Z and U.

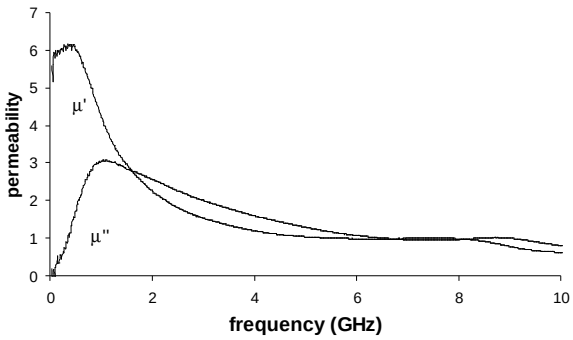

Fig. 7. Permeability spectra of the ZU composite sintered at 1300 °C.

Fig. 8 shows the μ spectra of a ZW composite. An increase in magnetic losses and μ" around 1 GHz can be observed. This can be attributed to the DWR of both hexaferrites and to the FMR of the Z-hexaferrite since the FMR frequency of CoW-hexaferrite was reported above 10 GHz [10,12]. Therefore, the increase in the μ" due to the FMR of the W-hexaferrite could be expected above the measured frequency range. The μ_i at 40 MHz is 6.2. For the W-hexaferrite μ_i = 2.1 was calculated from Equation (1). Here we have taken into an account the weight ratio of Z/W = 1.86 determined with the Rietveld method due to discussed limitations of the Pawley method. As mentioned previously, the μ_i of W-hexaferrite is similar to that of M-hexaferrite.

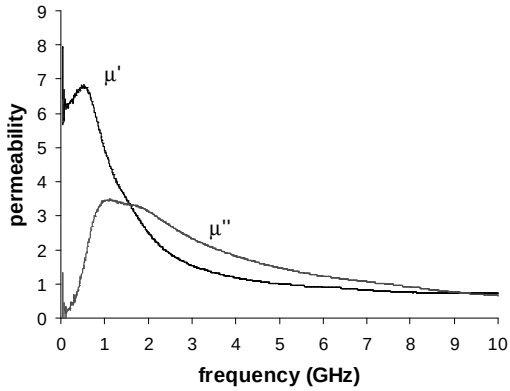

Fig. 8. Permeability spectra of the ZW composite sintered at 1300 °C.

4. Conclusions

We have prepared two types of composites using a solid-state reaction: spinel/hexaferrite (SM) and hexaferrite composites (ZU and ZW). The influence of the constituent phases on the μ and FMR of the composites was obvious. We have shown that the effective media theory can be applied for both types of composites since the difference in the μ of the constituent phases is significant. The agreement between the measured and calculated μ spectra of the SM composites was excellent. We can conclude that it is also possible to get some information about the composition of composites from the μ spectra if we take into account the microstructure of the composites. The effective media approach was also compared with the established X-ray methods for the quantitative phase determination based on: i) the integral intensities of the peaks based on the Pawley method and ii) the Rietveld method. It was shown that all three methods were more or less reliable as long as we are aware of their limitations.

Acknowledgement

This work was supported by the Ministry of Higher Education, Science and Technology of Republic of Slovenia.

References

[1] M. Pardavi-Horvath, J. Magn. Magn. Mater. **215-216**, 171 (2000).
[2] G. P Rodrigue, IEEE Trans. Microwave Theory Tech. **MTT-11**, 351 (1963).

[3] J. Smit, H. P. J. Wijn, Ferrites, Philips' Technical Library, Eindhoven, (1959).
[4] V. B. Bregar, Phys. Rev. B **71**, 174418 (2005).
[5] H. M. Rietveld, Acta Cryst. **22**, 151 (1967).
[6] G. S. Pawley, J. Appl. Cryst. **14**, 357 (1981).
[7] M. A. Vinnik, A. I. Aragonavskaya, N. N. Semenova, Rus. J. Inorg. Chem. (Transl. Z. Neorg. Chim.), **12**, 18 (1967).
[8] V. B. Bregar, D. Lisjak, A. Znidarsic, M. Drofenik, submitted to J. Eur. Ceram. Soc.
[9] N. Hiratsuka, R. Ikeda, R. Wada, K. Kakizaki, Proceedings of The Eight International Conference on Ferrites (ICF 8), Kyoto and Tokyo, Japan, 2000, p. 939.
[10] R. C. Pullar, S. G. Appleton, A. K. Bhattcharya, J. Mater. Sci. Lett. **17**, 973 (1998).
[11] D. Lisjak, P. McGuiness, M. Drofenik, submitted to Chem. Mat.
[12] C. Sudakar, G. N. Subbanna, T. R. N. Kutty, J. Appl. Phys. **94**, 6030 (2003).

*Corresponding author: darja.lisjak@ijs.si